

SNS RING OPTICS TUNING*

J.A. Holmes, W. Wan, SNS, ORNL, Oak Ridge, TN 37831-6473, USA
 N. Catalan-Lasheras, A. Fedotov, I. Papaphilippou, and J. Wei BNL, Upton, NY 11973, USA

Abstract

Detailed studies of the SNS ring lattice optics have been conducted. The horizontal and vertical tuning ranges for matched solutions with well-behaved lattice functions were determined and the power supply margin verified. Using stability criteria, potential working points have been identified and studied in detail. Studies, focused on behavior of the lattice functions under increasingly complex assumptions, included chromatic effects and sextupoles, and lattice perturbations due to injection chicane and to dynamic bumps for painting. Results are being used in determining injection painting schemes, in dynamic aperture studies, and in validating collimator settings.

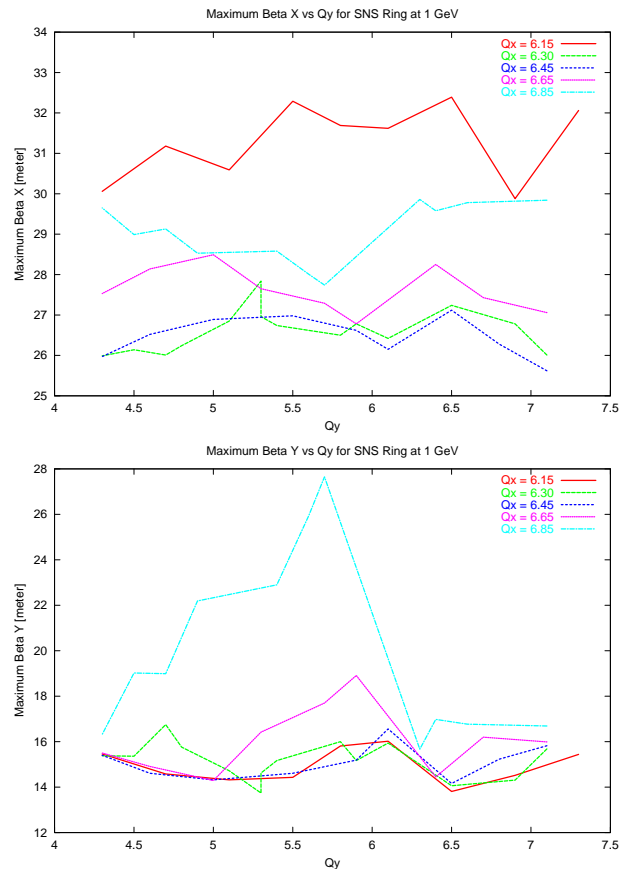
1 INTRODUCTION

The SNS accumulator ring will compress a 1 msec high intensity proton beam from a linac into a $1 \mu\text{sec}$ bunch for delivery to a mercury target. The compressed bunch will contain in excess of 10^{14} protons, and uncontrolled losses cannot exceed 10^{-4} . These constraints of high intensity and low losses place stringent requirements on the ring design. The SNS ring contains four superperiods, each consisting of a 90° arc and a straight section. The four straight sections each perform a distinct function: injection, collimation, extraction and gap kicker, and RF. In order to provide sufficient room for this, each straight sections consists of two doublets separated by a 12.5 m drift, and two 6.85 m drifts between the doublets and the arcs. To guarantee zero dispersion in the straight sections, each arc is an achromat consisting of four fodo cells. The SNS ring lattice was designed for a 1 GeV proton beam and can accommodate a 1.3 GeV beam with minor changes [1]. The circumference of the ring is 248 m.

In order to carry out the detailed design of the accumulator ring, it is first necessary to study the beam optics. We have carried out many of these basic calculations, using the MAD Code [2], and the results are presented here. In particular, we first determine the accessible tune space having matched lattice functions and acceptable magnet field strengths. From this we select potential working points for further study. We then examine off-momentum particles to assess dispersion effects, add the injection chicane and bump magnets and show that these lead to some degree of beta beating, include chromaticity sextupoles, and finally look at the effects of certain magnet errors.

2 RESULTS

In order to determine the accessible region of tune space, we have a number of degrees of freedom and some constraints. Constraints include the necessity of matched solutions, beta functions within aperture-dictated limits, magnet field strengths within specifications, and achromatic arcs. Degrees of freedom include the phase advances in the straight sections and the vertical phase advance in the arcs. The horizontal phase advance in the arcs is restricted to 2π by the achromaticity constraint. The accessible region of tune space for the SNS ring lattice ranges from $6 < Q_x < 7$ and $4 < Q_y < 7$. Figure 1 shows the behavior of the maxima of the lattice functions β_x, β_y, D_x and of the doublet focusing quadrupole strength as a function of Q_y for different values of Q_x . Considerations of these and other parameters aided in our definition of the accessible tune space.



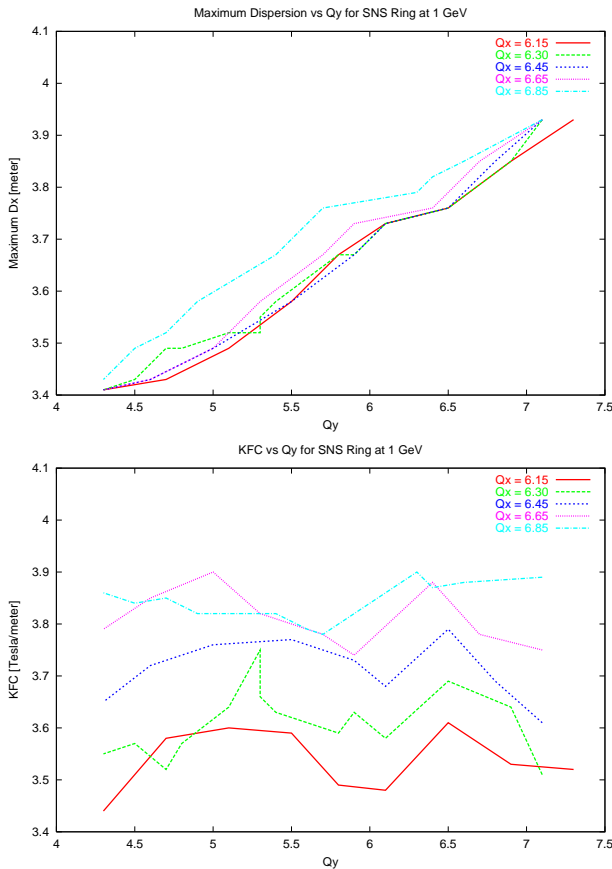


Figure 1. Parameters found in tune space survey.

For tunes above 7, some magnet strengths exceed specifications and beta functions exceed limits. For tunes below the specified ranges, there is insufficient focusing for solutions to be obtained. Within this range there are also inaccessible gaps due to structure resonances. These occur around $Q_x, Q_y = 6$, which is a second order structure resonance and also as Q_y approaches 4, which is a first order structure resonance. As a tune approaches one of these structure resonance values, the corresponding beta functions become excessive, and sufficiently close to the resonance no solutions exist. Particularly severe is the case of Q_x approaching 6. Because of the achromatic constraint, the horizontal phase advance is fixed in the arcs, and an excessive change in the rate of phase advance between arc and straight sections causes β_x to become too large at the injection foil by the time $Q_x = 6.15$. Because the rate of vertical phase advance can be kept more uniform throughout the ring, the effect when Q_y is in the vicinity of the vertical resonant regions is more localized. However, we follow the practice of keeping both Q_x and Q_y well removed from these integer values.

Selection of potential operating points from this large region in tune space becomes simpler with the aid of a resonance analysis. To start, we consider the most dangerous resonances: first and second order resonances, third order structure resonances, and fourth order structure sum resonances. In horizontal tune space, there is a second order resonance at $Q_x = 6.5$ and a third order

structure resonance at $Q_x = 6.67$. Given the tune spread of the intense SNS beam ($\Delta Q \approx 0.2$), avoidance of these resonances requires choosing $6.15 < Q_x < 6.5$. For the same reason, we must also choose $Q_y < 6.5$. Analysis of the vertical tune space reveals only two regions with working space between resonances at this level: $4 < Q_x < 4.5$ and $6 < Q_x < 6.5$. Of these, the vertical beta functions are better behaved in the second region, so we concentrate on operating points in the region $6.15 < Q_x, Q_y < 6.5$. Figure 2 shows this region including all resonance lines to fourth order and two potential operating points. Of these, the point at $(Q_x, Q_y) = (6.4, 6.3)$ is further removed from the second order structure resonance at 6.0, but nearby third and fourth order sum resonances may require correction to prevent beam loss. The point at $(Q_x, Q_y) = (6.23, 6.2)$ avoids the higher order resonances, but at high intensities the tune spread may excite the structure resonance at 6.0. Both of these operating points are being subjected to full beam dynamic studies [3-5].

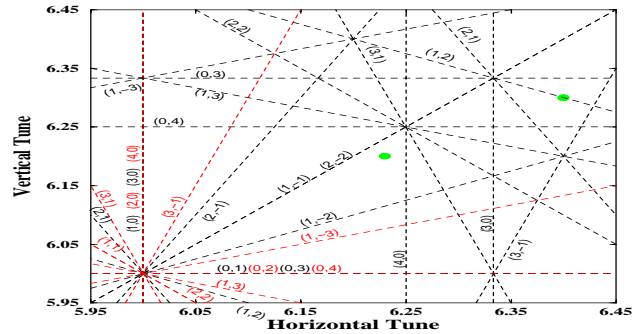


Figure 2. Potential operating points in tune space. All resonance lines through fourth order are shown.

Because these two operating points are reasonably close in tune space, their lattice functions are quite similar. The horizontal and vertical beta functions both peak at the doublets in the straight sections, at approximately 27 m and 15 m, respectively; and the dispersion in the arcs peaks at about 3.7 m. At the injection foil, however, the beta values are $(\beta_x, \beta_y) = (7.2 \text{ m}, 11.0 \text{ m})$ for the (6.4, 6.3) operating point and $(\beta_x, \beta_y) = (10.4 \text{ m}, 12.2 \text{ m})$ for the (6.23, 6.20) operating point. Thus, the injection painting scheme must be optimized independently for each operating point. The horizontal and vertical chromaticities are about -8 and -7 , respectively.

Consequently, for $\frac{\Delta p}{p_0} = \pm 0.01$, which corresponds to

$\Delta E \approx \pm 15 \text{ MeV}$ for 1 GeV protons, the closed orbit deviation reaches 37 mm in the arcs and about 1-2 mm in the straight sections, and the horizontal and vertical tunes are shifted by about -0.08 and -0.07 , respectively.

The injection chicane consists of four static horizontal dipole magnets in one of the 12.5 m straight section drifts

and eight dynamic bump magnets (four horizontal, four vertical) arrayed symmetrically in the corresponding 6.85 m drifts. When the static injection dipoles are included in the ring lattice, the horizontal closed orbit is bumped about 10 cm in the injection region. This bump leads to a local blip, also of 10 cm, in the dispersion function and beta-beating of about 5% in β_y at the doublets. When the dynamic bump magnets are activated, the beta-beating is not strongly affected, but now there is a residual dispersion function around the ring. In the case of a large bump (40 mm in x and 46 mm in y – sufficient to direct the closed orbit through the foil), the residual horizontal dispersion peaks at 25 cm in the straight section doublets and there is a vertical dispersion function of up to 15 cm

distributed around the ring. For $\frac{\Delta p}{p_0} = \pm 0.01$ the horizontal closed orbit deviation reaches about 6 mm and the vertical closed orbit deviation reaches about 1.5 mm in the straight sections.

The corrector magnets include four sets of chromatic sextupoles in the arc sections. With these sextupoles activated and set to eliminate the first order chromaticities and the variation of the beta functions, the main effect is the reduction of the chromaticities to near zero. The tunes remain essentially constant (variation < 0.01) for particles

with $\frac{\Delta p}{p_0} = \pm 0.01$. The effect of eliminating the variation of the beta functions with energy is to make the ring

maximum beta function values at $\frac{\Delta p}{p_0} = 0$ minima when plotted versus energy. In spite of eliminating the first order energy variation, the maximum beta function values

at $\frac{\Delta p}{p_0} = \pm 0.01$ typically exceed those at $\frac{\Delta p}{p_0} = 0$ by a few percent, and for one case, the (6.23, 6.20) operating point, the increase in maximum β_x is 20%.

The effects of magnet errors are also being studied. One example involves the large arc quadrupoles, which are located at the maxima in the dispersion function and which accordingly have 26 cm, rather than 21 cm, bore radii. Introducing random errors, using a Gaussian distribution of 0.4% width and truncated at 1% maximum error, into these magnets results in beta-beating of about 4% in β_x and in an increase in the maximum of the horizontal dispersion function from 4.00 m to 4.35 m for the (6.23, 6.20) operating point. Because these are focusing quadrupoles, the vertical lattice functions are unaffected by the errors. To avoid these errors, the large arc quadrupoles will be placed on their own separate power supply.

Another possible source of error would be a dynamic mismatch of the injection kicker strengths. We considered an extreme worst case situation of 1% errors in the kicker

field strengths at the large kick size of 40 mm in x and 46 mm in y. The errors were assigned systematically to maximize their effect. The result was a mild closed orbit distortion of 1.6 mm distributed around the ring. Thus, the control of the beam painting afforded by the kickers will be good.

3 SUMMARY

Serious beam optics studies have been conducted for the SNS ring lattice in order to assess the tuning ranges, potential working points, behavior of the lattice functions, chromatic effects and sextupoles, and lattice perturbations due to injection chicane and dynamic bumps. Although the lattice can be tuned to a broad range of satisfactory solutions, stability considerations for the intense SNS beam strongly limit the selection of potential working points. Of the two candidate working points, that at $(Q_x, Q_y) = (6.4, 6.3)$ may require correction to prevent beam loss due to nearby third and fourth order resonances, while that at $(Q_x, Q_y) = (6.23, 6.2)$ is near the limit of approach to the structure resonance at 6.0. The static dipoles in the injection chicane cause beta-beating at an acceptable 5% level, while the dynamic bump magnets result in both horizontal (0.25 m) and vertical (0.15 m) residual dispersion in the straight sections. The four families of chromatic sextupoles in the arcs can correct the chromaticity to near zero and remove the first order energy variations in the beta function maxima. The optics effects of some specific magnet errors have also been investigated. The results of these studies are now being used in determining injection painting schemes, in dynamic aperture studies, and in validating collimator settings.

4 ACKNOWLEDGEMENTS

Research on the Spallation Neutron Source is sponsored by the Division of Materials Science, U.S. Department of Energy, under contract number DE-AC05-96OR22464 with UT-Battelle Corporation for Oak Ridge National Laboratory.

5 REFERENCES

- [1] J. Wei, "Preliminary Change Request for the 1.3 GeV- Compatible Ring," BNL/SNS Technical Note 076, (Brookhaven National Laboratory, 2000).
- [2] H. Grote and F. C. Iselin, "The Mad Program (Version 8.19) User's Reference Manual, CERN/SL/90-13 (AP), (CERN, Geneva, Switzerland, 1996).
- [3] A. Fedotov, N. Malitsky, Y. Papaphilippou, J. Wei, and J. Holmes, PAC 2001, Paper RPAH004, (Chicago, 2001).
- [4] Y. Papaphilippou, A. Fedotov, N. Malitsky, A. Shishlo, and J. Wei, PAC 2001, Paper TPPH008, (Chicago, 2001).
- [5] J. Wei, J. Beebe-Wang, J. Brodowski, A. Fedotov, C. Gardner, Y. Lee, D. Raparia, V. Danilov, J. Holmes, C. Prior, G. Rees, and S. Machida, PAC 2001, Paper WPPH050, (Chicago, 2001).